Spin vector deviation and the gravitational wave memory effect between two free-falling gyroscopes in the plane wave spacetimes

Ke Wang and Chao-Jun Feng*

Division of Mathematical and Theoretical Physics, Shanghai Normal University, 100 Guilin Road, Shanghai 200234, People's Republic of China

(Received 6 February 2023; accepted 30 March 2023; published 26 April 2023)

In plane wave spacetimes, we find that there will be a precession angle deviation between two free-falling gyroscopes when gravitational waves passed through. This kind of angle deviation is closely related to the well-known standard velocity memory effect. Initial conditions such as the separation velocity or displacement between the two gyroscopes will affect this angle deviation. This result might be understood as a special relativistic consequence of the velocity memory. The evolutions of the angle deviation are calculated for different cases. We find that in some extreme circumstances, the angle deviation's order of magnitude produced by a rotating compact binary source could be 10^{-14} rads. Therefore, this memory effect caused by the gravitational wave is likely to be detected in the future.

DOI: 10.1103/PhysRevD.107.084044

I. INTRODUCTION

After decades of exploration, the gravitational waves (GWs) from a binary black hole merger were successfully detected in 2016 [1,2], which marked the arrival of the era of multimessenger astronomy.

Gravitational wave memory arises from the nonoscillating components of gravitational waves. The research on memory effects can be traced back to 1974 [3]. Zel'dovich and Polnarev claimed that the distance between a pair of test masses should be changed by gravitational waves. Further studies have shown that gravitational waves can also cause the relative velocity change between the two test masses [4]. These early discovered memory effects are now commonly considered as ordinary memory since they are all produced by the final state of the gravitational wave source. In 1991, Christodoulou *et al.* found that the effective energy radiated in gravitational waves would also produce memory effects, which are generally referred to as nonlinear memory or null memory of gravitational waves [5,6]. Later calculations in the post-Newtonian (PN) approximation [7–9] and numerical relativity [10,11] also support the existence of null memory effect.

The essence of null memory is that the passage of gravitational waves (or "soft gravitons") causes permanent changes in spacetime, resulting in various observable phenomena. Up to now, a lot of distinct manifestations of gravitational memory have been predicted by theoretical calculation, among which the most classic and most studied is known as displacement memory [11,12], which is described as the permanent change of distance between a pair of free-falling test particles after the gravitational wave passes through. Other known memory effects include velocity memory [4,13], spin memory [14,15], center-of-mass memory [16], and recently gyroscopic memory [17]. The aim of this paper is to reveal a new manifestation of gravitational memory, which is closely related to the velocity memory effect.

A more profound perspective on these memory effects is the correlation with the symmetry group of asymptotically flat spacetime, the Bondi-Metzner-Sachs (BMS) group [18,19]. Strominger *et al.* used an infrared triangle to depict the corresponding relationship between memory effects and the soft theorem and the symmetries of null infinity [20,21]. In recent years, numerous studies on BMS group and its extensions have linked various memory effects to various asymptotic conserved charges [15,21–23]. These insights into gravity symmetry may open the way to the quantization of gravity.

We shall work in nonlinear plane gravitational wave spacetimes, although memory effects have been studied frequently in asymptotically flat spacetimes. As a distant local approximation to general gravitational waves, plane waves retain most of the local properties of gravitational waves and are formally easier to calculate. The main research objects in this paper are a pair of separated test gyroscopes placed far away from the source, whose back-reaction to gravitational waves is negligible. By a natural way of comparing two separated gyroscopes, we express the deviation of the two gyroscopes as a relative angle, which is motion independent and invariant in flat spacetimes. Through direct calculation, we show that gravitational waves will permanently change the angle deviation

*Corresponding author.
fengcj@shnu.edu.cn

between the two gyroscopes, that is, the gravitational memory effect. Remarkably, the angular deviation between the gyroscopes naturally corresponds to the velocity memory effect in plane gravitational wave spacetimes. This peculiarity may motivate some novel proposals for detecting gravitational memory. Moreover, as a corollary to our calculation, we will discuss the dynamics of a single gyroscope in nonlinear plane wave spacetimes and compare it to the known gyroscopic memory in asymptotic flat spacetimes [22], which might be helpful to delimit the applicable scope of plane gravitational waves.

The paper is organized as follows: Sec. II reviews the general formalism for exact plane gravitational wave spacetimes and the geodesic motion and memory effect in it. In Sec. III, we first describe the kinematics of gyroscopes in plane wave spacetimes, after which we give the precession equations of the free-falling gyroscope with respect to a local tetrad and discuss the differences from the results in asymptotically flat spacetimes. Next, we focus on the two separated gyroscopes. After illustrating how two observers at different locations with different speeds can compare the gyroscopes they carry, we display the permanent angle deviation between the two gyroscopes generated by gravitational waves. At the end of Sec. III, we discuss the effects of separation distance and separation velocity on the deviation angle under a toy model, respectively. Finally, in Sec. IV, we estimate the amplitude of angle deviation generated by compact binary gravitational wave sources.

Notation.—Throughout this paper, we use geometric units in which $c = G = 1$. Greek letters $(\mu, \nu, \ldots)$ denote the spacetime indices and the range of available values is (0, 1, 2, 3), Latin indices $(a, b, \ldots)$ denote the coordinates indices of the plane of vibration, and the available values is (2, 3). Hatted letters $(\hat{\mu}, \hat{\nu}, \ldots)$ are internal Lorentz indices associated with a local frame established in Sec. III A. Capital bold letters represent vectors or matrices and will be explained again after it appears. All the dots above the letters in this paper represent the derivative with respect to U unless otherwise stated.

II. EXACT PLANE GRAVITATIONAL WAVE SPACETIMES

This section briefly reviews the metric of general plane wave spacetimes and the geodesic motion and memory effects in it.

A. Metric

Plane gravitational wave spacetime is commonly described in Baldwin-Jeffery-Rosen (BJR) coordinates (u, v, x^1, x^2) or Brinkmann coordinates (U, V, X^1, X^2) [12,24]. The general form of metric in BJR coordinates is

$$g = a_{ij} dx^i dx^j + 2du dv, \tag{1}$$

where the x^i $(i = 1, 2)$ are coordinates on the plane of vibration, the matrix $\boldsymbol{a}$ with component $a_{ij}(u)$ are symmetric and positive. In this form, the familiar linearized transverse traceless (TT) gauge can be expressed as $a_{ij} = \delta_{ij} + h_{ij}^{\mathrm{TT}}$, [12] shows that the BJR coordinates have coordinate singularities, which are typically not global, while the Brinkmann coordinates are the global coordinates of plane wave spacetime, and the metric is written as

$$g = 2dUdV + \delta_{ij} dX^i dX^j + DdU^2, \tag{2}$$

where D is a scalar function of coordinates (U, X^1, X^2) with the form of

$$\begin{aligned} D &= K_{ij}(U) X^i X^j \\ &= \frac{1}{2} A_+(U)((X^1)^2 - (X^2)^2) + A_\times(U) X^1 X^2, \end{aligned} \tag{3}$$

where $A_+(U)$ and $A_\times(U)$ are the amplitude of the $+$ and $\times$ polarization state. The nonzero components of the Riemann curvature tensor are $R_{iUjU} = -K_{ij}(U)$, and the only nonvanishing component of Ricci tensor is $R_{uu} = -K_{22} - K_{11} = -\mathrm{Tr}(K)$. Therefore, when $\boldsymbol{K}$ is traceless, the metric in Brinkmann coordinates strictly satisfies the vacuum Einstein field equation, that is, the spacetime is Ricci flat.

There is a transformation relationship between BJR (1) and Brinkmann (2) coordinates, which can be expressed as

$$\begin{cases} U = u \\ \boldsymbol{X} = \boldsymbol{P}(u)\boldsymbol{x} \\ V = v - \frac{1}{4}\boldsymbol{x} \cdot \dot{\boldsymbol{a}}(u) \cdot \boldsymbol{x} \end{cases} \quad \text{with} \quad \begin{cases} \boldsymbol{a} = \boldsymbol{P}^T \boldsymbol{P} \\ \ddot{\boldsymbol{P}} = \boldsymbol{K}\boldsymbol{P} \\ \boldsymbol{P}^T \dot{\boldsymbol{P}} = \dot{\boldsymbol{P}}^T \boldsymbol{P} \end{cases}, \tag{4}$$

where bold letters $\boldsymbol{X}$ and $\boldsymbol{x}$ represent column vectors composed of two coordinates of the plane of vibration, and all the other bold types represent the 2×2 matrix. Note that to get an explicit coordinate transformation one still has to solve a second-order ordinary differential eqution (ODE) of $\boldsymbol{P}$, which is $\ddot{\boldsymbol{P}} = \boldsymbol{K}\boldsymbol{P}$. However, many interesting properties can still be analyzed using the above form [12]. Since $\boldsymbol{P}$ has one extra degree of freedom, the coordinate transformation is not a one-to-one mapping if the initial value of $\boldsymbol{P}$ is not chosen [24].

In fact, the Brinkmann coordinates (2) can be viewed as the local Lorentz coordinates of plane wave spacetimes [13], which makes the geodesic equation to some extent equivalent to the observed effect of the origin observer. In contrast to BJR coordinates, the geodesic motion in Brinkmann coordinates show rich observational effects of gravitational waves. Moreover, the Brinkmann coordinates also have computational advantages over BJR coordinates. Therefore, the following calculations in this paper will mainly use Brinkmann coordinates.

B. General geodesic motion

In this part, we rewrite the general solution of geodesic equations given by [25], but in a more concise form. First, we consider an arbitrary geodesic $\Pi(\tau)$ with tangent vector $\boldsymbol{u}$, the geodesic equation for coordinate U is

$$\frac{d^2U}{d\tau^2} = 0, \tag{5}$$

with initial value $U(\tau_0) = U_0$, and the general solution to Eq. (5) is

$$U = \gamma(\tau - \tau_0) + U_0, \tag{6}$$

where the parameter γ is a conserved constant along the geodesic $\Pi(\tau)$. If we use $\boldsymbol{l} = \partial_V$ to represent the normal vector of the null hypersurface parametrized by U, then $\gamma = \boldsymbol{u}\cdot\boldsymbol{l}$. Since there is a linear relationship between U and τ, we will use the coordinate U instead of the geodesic affine parameter τ in the rest of the paper. Then, the geodesic equation of the other three coordinates is as follows:

$$\ddot{\boldsymbol{X}} = \boldsymbol{K}(U)\boldsymbol{X}, \tag{7}$$

$$\ddot{V} = -\frac{1}{2}\dot{D} - 2\dot{\boldsymbol{X}}^T\boldsymbol{K}\boldsymbol{X}. \tag{8}$$

Hereafter the dot denotes the derivative with respect to U. After setting the initial coordinates as $x^\mu(U_0) = (U_0, V_0, \boldsymbol{X}_0)$, and the initial four velocity as $u^\mu(U_0) = \gamma(1, \dot{V}_0, \dot{\boldsymbol{X}}_0)$, the general solutions to Eqs. (7) and (8) are then obtained as[1]

$$\boldsymbol{X} = \boldsymbol{P}(U)\boldsymbol{X}_0 + (U - U_0)\boldsymbol{H}(U)\dot{\boldsymbol{X}}_0, \tag{9}$$

$$V = V_0 - \frac{1}{2}\left(\boldsymbol{X}^T\dot{\boldsymbol{X}} - \boldsymbol{X}_0^T\dot{\boldsymbol{X}}_0 + \frac{1}{\gamma^2}(U - U_0)\right), \tag{10}$$

where $\boldsymbol{P}$ and $\boldsymbol{H}$ are both 2×2 matrices and they satisfy the following equations, respectively,

$$\ddot{\boldsymbol{P}} = \boldsymbol{K}\boldsymbol{P}, \qquad (U - U_0)\ddot{\boldsymbol{H}} + 2\dot{\boldsymbol{H}} = (U - U_0)\boldsymbol{K}\boldsymbol{H}, \tag{11}$$

with the boundary conditions $\boldsymbol{P}(U_0) = \boldsymbol{H}(U_0) = \boldsymbol{I}$, $\dot{\boldsymbol{P}}(U_0) = \dot{\boldsymbol{H}}(U_0) = 0$. Note that $\dot{V}_0$ exists only in the constant γ, so the velocity in the direction of gravitational wave propagation has no effect on the motion of the vibration plane. Without losing generality, the following discussions will not consider the velocity of propagation direction but only the two-dimensional motion of the vibration plane.

Using the solutions (5), (9), and (10) we can easily write the proper velocity of general geodesic motion as

$$\boldsymbol{u} = \gamma\left(\partial_U - \frac{1}{2}\left[\frac{1}{\gamma^2} + \dot{\boldsymbol{X}}^T\dot{\boldsymbol{X}} + \boldsymbol{X}^T\boldsymbol{K}\boldsymbol{X}\right]\partial_V + (\dot{\boldsymbol{X}})^i\partial_{X^i}\right), \tag{12}$$

where

$$\dot{\boldsymbol{X}} = \dot{\boldsymbol{P}}\boldsymbol{X}_0 + ((U - U_0)\dot{\boldsymbol{H}} + \boldsymbol{H})\dot{\boldsymbol{X}}_0. \tag{13}$$

Thanks to the properties of the local Lorentz gauge, the geodesic equations (5), (7), and (8) in Brinkmann coordinates have the same form as the geodesic deviation equations of the geodesic that maintain $\boldsymbol{X} = 0$, so the solutions (6), (9), and (10) are also the solutions to the geodesic deviation equations, which makes it convenient for us to give the expressions of displacement memory and velocity memory. Before that, let us briefly review the memory effect in plane wave spacetimes.

C. Memory effect

We follow the common analytical methods, consider sandwich waves, that is, gravitational waves exist only for a zone like $U \in [U_i, U_f]$, while the spacetime of $U < U_i$ and $U > U_f$ are flat but not equivalent. The theoretical foundation of nonequivalence lies in the fact that the flat condition $R_{\mu\nu\alpha\beta} = 0$ does not constrain the linear evolutionary process of spacetime, or $K_{ij} = 0$ only implies $\boldsymbol{P}(U) = \boldsymbol{P}^0 + U\boldsymbol{P}^1$. In linear theory, it can be expressed as

$$R_{\mu\nu\alpha\beta} = 0 \Rightarrow h_{ij}(U) = h_{ij}^0 + Uh_{ij}^1, \tag{14}$$

where h_{ij}^0 and h_{ij}^1 are both constants. In fact, Eq. (14) only shows that the spacetime before and after the gravitational wave zone can be theoretically unequal. Using the Hamilton-Jacobi method in BJR coordinates, [12] shows that the spacetime before and after the gravitational wave zone are indeed not equivalent. In short, if we set $a_{ij}(U < U_i) = \delta_{ij}$, we can get

$$a_{ij}(U > U_f) \approx \delta_{ij} + 2\int_{U_i}^{U_f} du' \int_{U_i}^{u'} R_{i0j0}(u'')du' \tag{15}$$

at the linear level. This is the physical essence of the gravitational wave memory effect, the spacetime changes permanently after the passage of the pulse. This inequivalence of spacetime before and after zone will be discussed again in Sec. III.

[1] Note that the solutions (9) and (10) are only formal solutions, because Eq. (11) is still an unavoidable Sturm-Liouville problem about second-order ODE [26].

Consider a static test particle with initial coordinates $\boldsymbol{X}_0$ and using the solutions (9) of the geodesic equations, the change in position after the passage of a gravitational wave can be written as

$$\Delta \boldsymbol{X} = (\boldsymbol{P}(U_f) - \boldsymbol{I})\boldsymbol{X}_0, \tag{16}$$

which is a general form of displacement memory in our notation. There is more consideration about velocity memory since the initial position $\boldsymbol{X}_0$ and the initial velocity $\dot{\boldsymbol{X}}_0$ can be taken into account simultaneously. Using Eq. (13), the change in velocity can be written as

$$\Delta \boldsymbol{V} = \dot{\boldsymbol{P}}\boldsymbol{X}_0 + ((U_f - U_0)\dot{\boldsymbol{H}} + \boldsymbol{H} - \boldsymbol{I})\dot{\boldsymbol{X}}_0, \tag{17}$$

which is a general form of velocity memory in our notation. See Eq. (11) in the previous section for the definitions of matrices $\boldsymbol{P}$ and $\boldsymbol{H}$.

At present, the known manifestations of memory effect are far more than the above two. Looking for more manifestations of memory effect will provide additional possible methods for detecting gravitational memory effects. In Sec. III, we will show a new manifestation of memory effect by studying the two separated spin vectors.

III. PRECESSION DEVIATION OF SPIN VECTORS

In this section, we study the evolution of the spin vectors in general plane wave spacetimes. The first step is to construct a local tetrad so that we can study the evolution in a three-dimensional framework. With this framework, we first discuss the precession of a free-falling gyroscope with respect to its own internal tetrad. After that, we describe a method of comparing two separated gyroscopes, which is then used to study the precession difference between the two separated gyroscopes due to gravitational waves. And finally, our results are discussed under a simple gravitational wave model.

A. Spin vector evolution of gyroscopes

Consider a free-falling observer with four velocity $\boldsymbol{u} = u^\nu \partial_\nu$ while carrying a gyroscope, the gyroscopic spin vector $\boldsymbol{S}$ obeys Fermi-Walker transport $(\boldsymbol{u}\cdot\nabla \boldsymbol{S})^\mu = (u^\mu a^\nu - u^\nu a^\mu)S_\nu$, and always satisfy $\boldsymbol{S}\cdot\boldsymbol{u} = 0$. If we construct a local tetrad $\{\boldsymbol{e}_{\hat\mu}\}$ of the observer by making $\boldsymbol{e}_{\hat 0} = \boldsymbol{u}$, and $\boldsymbol{e}_{\hat\mu}\cdot\boldsymbol{e}_{\hat\nu} = \eta_{\hat\mu\hat\nu}$, then the spin vector is purely spatial in the tetrad, and the precession equation of the three spatial components $S^{\hat i} = \boldsymbol{S}\cdot\boldsymbol{e}_{\hat i}$ (hereafter $i = 1, 2, 3$) can be deduced as [17]

$$\frac{dS^{\hat i}}{d\tau} = -u^a \omega_a^{\hat i\hat j} S_{\hat j} = \Omega^{\hat i}_{\hat j} S^{\hat j} \quad \text{with} \quad \omega_a^{\hat i\hat j} = \boldsymbol{e}^{\hat i}_\mu \nabla_a \boldsymbol{e}^{\hat j\mu}, \tag{18}$$

where $\boldsymbol{\omega}^{\hat i\hat j}$ is the spin connection one-form associated with the tetrad $\{\boldsymbol{e}_{\hat\mu}\}$, and $\boldsymbol{\Omega}$ can be considered as a 2-form of angular velocity.[2] To calculate $\boldsymbol{\Omega}$, we need to build a local tetrad for any timelike observer in a plane wave spacetime. The four velocity in Brinkmann coordinates (2) can be generally written as[3]

$$\boldsymbol{u} = \gamma(1, v^1, v^a) \quad \text{with}$$
$$\boldsymbol{u}\cdot\boldsymbol{u} = -1 \quad \text{and} \quad \gamma = (-D - 2v^1 - v^a v_a)^{-1/2}. \tag{19}$$

First, we set $\boldsymbol{e}_{\hat 0} = \boldsymbol{u}$, then subtract the part parallel to $\boldsymbol{e}_{\hat 0}$ from $\boldsymbol{l} = \partial_V$ to get $\boldsymbol{e}_{\hat 1}$. Since the vector $\boldsymbol{l} = \partial_V$ is tangent to outgoing null rays, $\boldsymbol{e}_{\hat 1}$ is related to the propagation direction of gravitational waves. And finally, we use the Gram-Schmidt orthogonalization procedure to get $\boldsymbol{e}_{\hat a}$. The whole tetrad is

$$\begin{aligned} \boldsymbol{e}_{\hat 0} &= \boldsymbol{u}, \\ \boldsymbol{e}_{\hat 1} &= \frac{1}{\gamma}\boldsymbol{l} + \boldsymbol{u}, \\ \boldsymbol{e}_{\hat a} &= \partial_a - v^a \boldsymbol{l}. \end{aligned} \tag{20}$$

Then, for the general timelike motion in Brinkmann coordinates, the spin connection can be calculated by using Eqs. (18) and (20) as follows:

$$\begin{aligned} \omega_\nu^{\hat a\hat b} &= 0, \\ \omega_\nu^{\hat 1\hat a} &= -\gamma\partial_\nu v^a + \gamma\Gamma^1_{\nu b}\delta^{ab}. \end{aligned} \tag{21}$$

By contracting the spin connection with four-velocity $\boldsymbol{u}$, we find two nonvanishing components of angular velocity $\Omega^{\hat i\hat j}$, they are

$$\Omega^{\hat 1\hat a} = \gamma(u^\nu\partial_\nu v^a - u^\nu\Gamma^1_{\nu b}\delta^{ab}). \tag{22}$$

B. Free-falling observer

We now discuss the gyroscopic precession that a free-falling observer carrying a gyroscope might observe. First, we compute the angular velocity of the free-falling gyroscope with respect to the local tetrad (20), the four velocity of general geodesic motion is given in Eq. (12), then using

[2]The antisymmetric tensor $\Omega^{\hat i}_{\hat j}$ can be dualized into a vector $\Omega^{\hat i} = -\frac{1}{2}\epsilon^{\hat i\hat j\hat k}\Omega_{\hat j\hat k}$, then the precession equation (18) can be simplified to $\dot{\boldsymbol{S}} = \boldsymbol{\Omega}\times\boldsymbol{S}$.

[3]Because we are working in U V coordinates, (v^1, v^a) here does not represent the three-dimensional velocity. The four velocity that includes three-dimensional velocity should be set as $\boldsymbol{u} = \beta(1 - v^r, -1 + v^r, v^a)$, which is more reasonable, but the calculation will be more complicated. According to our analysis in Sec. II B, the velocity in the propagation direction of the wave does not affect the motion of the plane of vibration, so we do not consider the velocity in the propagation direction of the wave, that is, $v^1 = -1$, then v^a can be regarded as the two-dimensional velocity. Still writing v^1 instead of -1 here just to keep generality.

the precession angular velocity (22), we find that $\Omega^{\hat{i}}_{\ \hat{j}} = 0$ (see Appendix A for a detailed calculation). It then follows from Eq. (18) that

$$\frac{dS^{\hat{i}}}{d\tau} = 0. \tag{23}$$

Accordingly, the spin vector component associated with the local tetrad (20) remains unchanged, which means that a free-falling observer carrying a gyroscope cannot detect the plane gravitational waves by observing the precession of the gyroscope.

In asymptotically flat spacetimes, both the displacement memory and velocity memory effects appear at order $\mathcal{O}(1/r)$ [27], where r denotes the distance to the source. The gyroscopic memory associated with spin memory appears at order $\mathcal{O}(1/r^2)$ [15,17], and the radial kick memory arises at $\mathcal{O}(1/r^3)$ [28]. These gravitational memory effects all correspond to asymptotic charges generated by particular asymptotic symmetries [28].

In nonlinear plane wave spacetimes, both the displacement memory and velocity memory effects appear at order $\mathcal{O}(h)$ [12,13], where h denotes the magnitude of wave tensors in standard TT gauge. Equation (23) shows that there is no gyroscopic memory in plane wave spacetimes. Moreover, the analysis of the geodesic equation (see Sec. II B) implies that there is no radial kick memory in plane wave spacetimes either. These "missing memories" reflect the fact that the information carried by plane waves is inherently incomplete. In the PN approximation, the leading order of the plane gravitational waveform h^{TT}_{ij} is $\mathcal{O}(1/r)$ [15]. Thus, at least on the scale of $\mathcal{O}(1/r)$, the prediction of memory effects in plane wave spacetimes is coincide with that in asymptotically flat spacetimes (the calculations for static observers in Appendix B also support this assertion). So we will keep the order of $\mathcal{O}(h)$ in the following calculations.

We now turn our focus on a pair of separated gyroscopes and it will show that gravitational waves create a permanent deviation among them. In the beginning, it is necessary to specify how two observers at different locations with different speeds can compare the gyroscopes that they carry. Since gyroscopic spin vectors are spatial for self-observer, given that parallel transport or Poincare transformation will alter the spatiality, we want a comparison between spatial vector and spatial vector so that the three-dimensional relative angle can be directly calculated. A natural idea is to move them together and have the same velocity, or to make their geodesics overlap, then the spin vectors can be compared in the same local tetrad. But for curved spacetimes, choosing different coincidence routes will give different results [29]. Fortunately, in flat spacetimes, the route can be arbitrary. We will show by a very brief calculation that the precession generated by an acceleration in a flat spacetime is path independent.

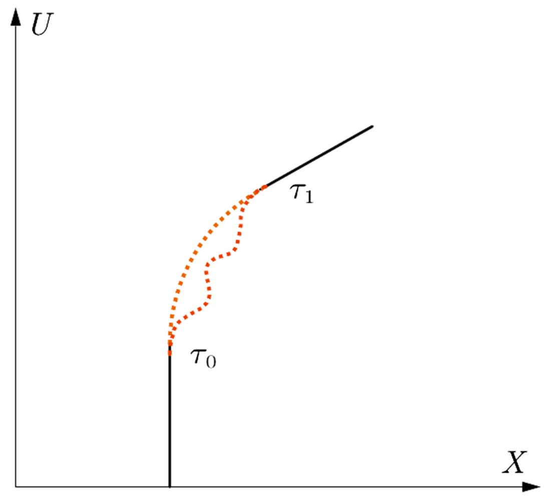

FIG. 1. A gyroscope moves along the worldline parametrized by τ. Outside the interval $[\tau_0, \tau_1]$ is geodesic motion. In Sec. III C, we show that no matter what acceleration process the gyroscope undergoes, as long as the starting and ending speeds are the same, the precession of the gyroscope associated with a local tetrad (20) will remain unchanged.

C. Path-independent precession angle

Consider a worldline $\aleph(\tau)$ in a Minkowski spacetime (see Fig. 1), make the acceleration section in $\tau \in [\tau_0, \tau_1]$, and we do not specify the acceleration, simply write the boundary conditions as

$$\left.\frac{d\boldsymbol{\aleph}}{d\tau}\right|_{\tau=\tau_0} = \boldsymbol{u}_0, \qquad \left.\frac{d\boldsymbol{\aleph}}{d\tau}\right|_{\tau=\tau_1} = \boldsymbol{u}. \tag{24}$$

In the Minkowski spacetime, the tetrad and the angular velocity are simply a special case of Eqs. (20) and (22). By taking $\boldsymbol{K} = 0$, the nonzero angular velocity reads

$$\Omega_{\hat{1}\,\hat{a}} = -u^\nu \gamma \partial_\nu v^a = -\gamma \frac{dv^a}{d\tau}. \tag{25}$$

Each component of the angular velocity (25) has a corresponding plane of rotation. For simplicity, we assume the acceleration is in the X^2 direction (while in general cases, one can always make the acceleration in the X2 direction by a rotational transformation), then the rotation angle in the $\boldsymbol{e}_{\hat{1}} \wedge \boldsymbol{e}_{\hat{2}}$ plane is obtained by integrating the angular velocity $\Omega_{\hat{1}\,\hat{2}}$ over the interval:

$$\theta = -\int_{\tau 0}^{\tau 1} \gamma \frac{dv^2}{d\tau} d\tau = -\int_{v_0^2}^{v^2} \gamma dv^2. \tag{26}$$

It shows that the precession angle is path independent, depending only on the starting and ending velocity. Given this property, it is clear how two observers with different speeds on different positions can compare the gyroscopes they carry. All it takes is for them to come together, or, to put it more precisely, make their worldlines overlap, and then we can compare them in the same tetrad. Obviously, this method is reasonable to apply in realistic scenarios. More generally, without deflection caused by force, the angle deviation of two gyroscopes is invariant as long as the spacetime remains flat no matter how they move. While the situation in curved spacetimes is much more complicated. For the method of how to compare the spin vectors in different positions in curved spacetimes, one can refer to the affine transport method given by [29].

D. Permanent angle deviation by separation

In Fig. 2, there are two gyroscopes G0 and G1 separated by a distance, where G0 is placed at the origin and G1 is placed at $\boldsymbol{X}_0 = (X_0^2, X_0^3)$. Their rotation direction is aligned at the beginning, and then they move along their geodesics respectively until the gravitational wave passes through. As shown in Sec. III B, each gyroscopic spin vector maintains its orientation within its local tetrad during geodesic movement. However, the local tetrad of G1 is no longer aligned with G0 because of the velocity memory effect. To compare the spin vectors of the two gyroscopes in our method of comparison, their worldlines should overlap. A simple choice is to accelerate G0 to the same velocity as

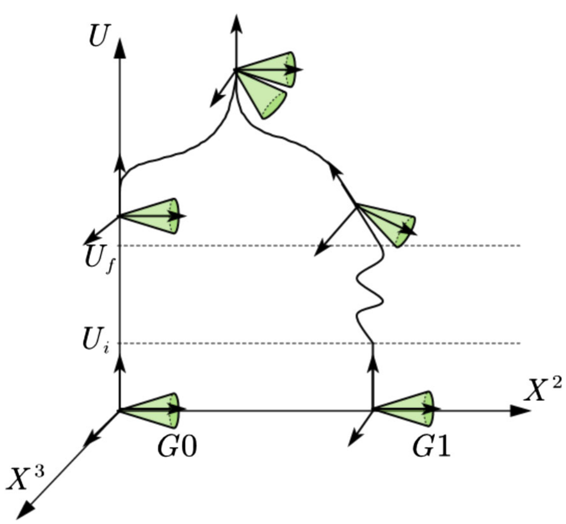

FIG. 2. The two nearby gyroscopes, G1 and G0, move along their worldliness in a plane wave spacetime, respectively. The picture is drawn in the Brinkmann coordinate system (2), while the coordinate V, which denotes the propagation direction of waves, is not shown in the picture. The region $[U_i, U_f]$ represents the spacetime location of the gravitational waves. The two gyroscopes are placed with the same orientation at the beginning. In the process of geodesic movement, each gyroscopic spin vector maintains its orientation in its local frame as shown in Sec. III B. After the burst, G1 and G0 are moved together through an arbitrary acceleration process, and at that time, the angle deviation between the two gyroscopes could be observed.

G1. First, accelerate G0 to $v_{\rm mem}^2$ in the X^2 direction and then to $v_{\rm mem}^3$ in the X^3 direction, where $v_{\rm mem}^a$ denotes the velocity memory of G1 relative to G0 in the X^a direction. According to Eq. (26), the precession angle of G0 in the $\boldsymbol{e}_{\hat{1}} \wedge \boldsymbol{e}_{\hat{a}}$ plane is calculated as

$$\theta^a = -\int_0^{v_{\rm mem}^a} (2-(v)^2)^{-1/2} dv = -\arcsin\left(\frac{v_{\rm mem}^a}{\sqrt{2}}\right). \quad (27)$$

In fact, Eq. (27) is the relative precession angle between two separated gyroscopes. As mentioned in Sec. III C, the precession angle is path independent, so without deflection caused by other forces, the angle deviation of the two gyroscopes will always exist after the wave passes through. This angle deviation reflects the in equivalence between the spacetime before and after the wave zone, which is exactly the memory effect between the two spin vectors.

Since the deviation angle (27) contains only the velocity memory $v_{\rm mem}^a$, it contains the same information as that of the standard velocity memory. Thus, the precession deviation between the two separate spin vectors is just a pattern of manifestation of the velocity memory. Note that this is only true for plane wave spacetimes, the deviation of two separated spin vectors in general gravitational wave spacetimes still needs further research.

Our results actually provide a way to observe the velocity memory effect statically. Consider two free-falling test masses, there will be a net change in the relative velocity between the two test masses after the passage of GWs, which is known as the velocity memory effect. Since the net change is dynamic and might be covered by the acceleration due to various forces, detecting it is a huge challenge. However, if we replace the two test masses with two test gyroscopes and observe the relative precession angle instead of the relative velocity after the passage of GWs, because the final precession angle is path independent as shown in Sec. III C, the observed precession angle deviation will remain the same when they are at relative rest.

E. Only the initial separation displacement

In this part, we will discuss the precession deviation with the only initial separation displacement, and in the next part, the initial separation velocity will be considered. Suppose that a detector consists of two gyroscopes and can compare the angle deviation in real time. A reasonable consideration is that there is only initial separation displacement between the two gyroscopes. Consider the simplest case, assuming that the initial separation is only in the X^2 direction and the separation distance is L. Since the initial separation speed is zero, the constant $\gamma = 1/\sqrt{2}$. Note that the gravitational wave region is $[U_i, U_f]$. By using Eq. (17), and $\boldsymbol{P} = \boldsymbol{I} + \frac{1}{2}\boldsymbol{h} + o(h^2)$ in linear theory with the transverse traceless gauge, we obtain the angle deviation at time U_f from Eq. (27):

$$\Delta\theta = \arcsin\left(\frac{1}{\sqrt{2}}\dot{P}_{22}(U_f)L\right) = \frac{1}{2\sqrt{2}}\dot{h}_+(U_f)L + o(h^2), \tag{28}$$

to avoid confusion, the matrix form of Eq. (28) is presented below,

$$\begin{pmatrix}\Delta\theta^2\\ \Delta\theta^3\end{pmatrix} = \arcsin\left(\frac{1}{\sqrt{2}}\begin{pmatrix}\dot{P}_{22} & \dot{P}_{23}\\ \dot{P}_{32} & \dot{P}_{33}\end{pmatrix}\begin{pmatrix}L\\ 0\end{pmatrix}\right) = \begin{pmatrix}\arcsin\left(\frac{1}{\sqrt{2}}\dot{P}_{22}(U_f)L\right)\\ 0\end{pmatrix}. \tag{29}$$

In this case, Eq. (28) shows that the angle deviation is approximately proportional to the initial separation distance L. In fact, the angle deviation at any time U in the region of $[U_i, U_f]$ could be given by

$$\Delta\theta(U) = \arcsin\left(\frac{1}{\sqrt{2}}\dot{P}_{22}(U)L\right) = \frac{1}{2\sqrt{2}}\dot{h}_+(U)L + o(h^2), \tag{30}$$

which is the evolution equation of the deviation angle in the gravitational wave region in the simplest case.

To show the evolution of the angle deviation, we calculate Eq. (30) in a toy model of the gravitational collapse [12], in which

$$A_+(U) = \frac{1}{2}\frac{d^3(e^{-U^2})}{dU^3} = \ddot{h}_+ + o(h^2). \tag{31}$$

The comparison between the linear approximation and the numerical simulation is shown in Fig. 3. The result shows that there is no final angle deviation in the linear approximation without any leading order velocity memory, while the numerical simulation demonstrates that there is an angle deviation when higher-order terms are taken into account.

The numerical simulation steps in this case are as follows: First, matrix $\boldsymbol{K}$ is given by model (31) and Eq. (3), then we numerically solve the differential equation (11) to produce matrix $\dot{\boldsymbol{P}}$, and finally substitute the matrix component $\dot{P}_{22}$ into the first part of Eq. (30) yields the numerical results.

F. Initial separation velocity

We now consider two gyroscopes with an initial separation velocity. Suppose that a detector can compare the precession angle between the two gyroscopes in real time

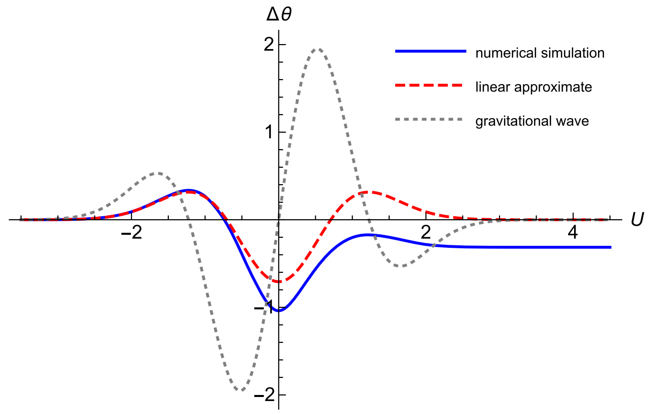

FIG. 3. Evolution of the deviation angle between two gyroscopes with initial separation displacement.

as they move along their geodesics. We assume that both the gyroscopes G0 and G1 are at the origin at the beginning, while G1 has the initial relative velocity v_0 along the X^2 direction. The final velocity of G1 after the gravitational wave passes through can be readily found from Eq. (17):

$$\begin{aligned} v &= ((U_f - U_0)\dot{H}_{22}(U_f) + H_{22}(U_f))v_0 \\ &= \left(1 - \frac{1}{2}h_+ + \frac{1}{2}(U_f - U_0)\dot{h}_+ + o(h^2)\right)v_0, \end{aligned} \tag{32}$$

in which we have used

$$\begin{aligned} (U - U_0)\boldsymbol{H} = (U - U_0)\boldsymbol{I} + \frac{1}{2}(U - U_0)\boldsymbol{h} \\ - \int_{U_0}^{U}\boldsymbol{h}dU + o(h^2). \end{aligned} \tag{33}$$

We also make G0 catch up with G1 to get the final angle deviation. By performing the same calculation as that in Eq. (28), one eventually finds that

$$\begin{aligned} \Delta\theta &= \arcsin\left(\frac{v}{\sqrt{2}}\right) - \arcsin\left(\frac{v_0}{\sqrt{2}}\right) \\ &= -\frac{1}{2\sqrt{2}}h_+(U_f)v_0 + \frac{T}{2\sqrt{2}}\dot{h}_+(U_f)v_0 + o(h^2), \end{aligned} \tag{34}$$

where $T = (U_f - U_i)$. Equation (34) shows that the angle deviation is proportional to the initial separation velocity at the leading order. We repeat the procedure of the previous part, first replacing U_f with U to estimate the angle deviation at any time, and then calculate the linear approximation and numerical simulation using the toy model (31). The evolution of $\Delta\theta$ is shown in Fig. 4.

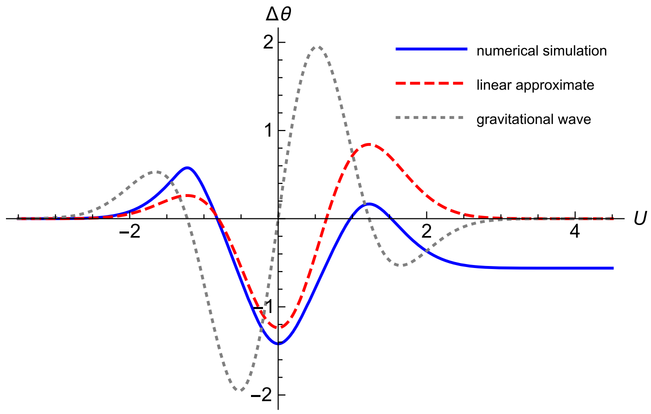

FIG. 4. Evolution of the deviation angle between two gyroscopes with initial separation velocity.

Consider a general case, there are both initial separation displacement and initial separation velocity between two gyroscopes. Equation (13) shows that the final velocity has a linear relationship with the initial separation displacement and velocity. Thus, the general angle deviation at the linear level is simply the addition of Eqs. (28) and (34), yielding

$$\Delta\theta = \frac{1}{2\sqrt{2}}(T\dot{h}_+^{\mathrm{mem}} - h_+^{\mathrm{mem}})v_0 + \frac{1}{2\sqrt{2}}\dot{h}_+^{\mathrm{mem}}L + o(h^2). \tag{35}$$

IV. ANGLE DEVIATION FROM COMPACT BINARY SOURCES

In this section, we specifically estimate the magnitude of angle deviation memory from compact binary sources (CBS). The leading-order memory waveform from CBS in the PN approximation is given by [15]

$$h_+^{\mathrm{mem}} = \frac{1}{48r}M\eta x_f \sin^2\theta(17+\cos^2\theta) + o(c^{-2}), \tag{36}$$

where M is the total mass of the binary and $\eta = m_1 m_2/M^2$, $x = (M\omega)^{2/3}$, where ω is the orbital frequency and m_1 m_2 are the masses of two components. The initial separation of two separated gyroscopes is assumed in the same direction as the + polarization direction. Restoring our results (35) to the standard unit yields

$$\Delta\theta = \frac{1}{2\sqrt{2}c}h_+^{\mathrm{mem}}v_0 + o(h^2), \tag{37}$$

where c denotes the speed of light. Since the memory term $\dot{h}_+^{\mathrm{mem}}$ of CBS disappears, the leading order term in Eq. (35) only contains the initial separation velocity v_0, while the contribution from the initial separation displacement is hidden in the higher order terms. Note that the plane wave approximation has a restriction on the initial separation velocity. If we use L_{max} to represent the maximum separation length allowed by the plane wave approximation and t_{d} to denote the gravitational wave duration, then the constraint of the initial separation velocity is $v \ll L_{\mathrm{max}}/t_{\mathrm{d}}$, or else the plane wave approximation will be invalid. Following the estimation of [13], L_{max} is about 10^{17} meters in the case of $v \ll c$. Assume that the two gyroscopes have an initial separation velocity close to the speed of light, then the maximum angle deviation between the two gyroscopes is estimated at about 10^{-14} rads. In such an extreme case, it requires a very short duration of gravitational waves, for instance, two supermassive black holes merge will emit a GW memory burst with an amplitude of 10^{-15} [30].

V. DISCUSSION

In this paper, we investigated the precession angle deviation between two separated free-falling gyroscopes in nonlinear plane wave spacetimes. We first show that a free-falling gyroscope maintains its orientation with respect to a local tetrad (20) in general plane-wave spacetimes, and it does not give the same results as that in the asymptotically flat spacetimes [17]. We then turn to discuss two separated gyroscopes. After illustrating how to compare the local observations of two gyroscopes in flat spacetimes, we find that gravitational waves will generate a permanent angle deviation between the two gyroscopes, and this kind of deviation is another manifestation of the well-known standard velocity memory effect. For compact binary gravitational wave sources, we expect to generate an angle deviation of about 10^{-14} rads between two gyroscopes under the most demanding conditions.

The guiding implications of our results for gravitational wave detection warrant further discussion. What we considered is that two gyroscopes move along their geodesics in the gravitational wave region, and then accelerate arbitrarily after the wave passes through to become relatively static. For real situations such as two separated gyroscopes placed on the ground-based detectors. For example, the test masses (mirrors) are replaced by the test gyroscopes in the detectors like LIGO and Virgo [31], and the detector's control system will counteract the velocity memory and then leave a permanent angle deviation between the test gyroscopes. Another way to detect such effects is to let the acceleration process occur in the gravitational wave region. For example, two gyroscopes connected by a straight rod without a complicated detector control system must have experienced nontrivial acceleration processes in the gravitational wave region to remain relatively static after the wave passed through. We will leave it to our next work.

It would be instructive to conceive of a large Sagnac interferometer [32], which is comparable in size and technique to LIGO. Based on the strain distance now accessible to LIGO, a large Sagnac interferometer might be able to sense the radian change of 10^{-25} rad. However, given the limitations of ground-based detection, it seems more promising to resort to a space-based gravitational-wave detector, such as the future LISA [33], which could be configured as a Sagnac interferometer [34]. If such interferometers are placed at different locations in space and we try to compare the strain differences accumulated during the passage of gravitational waves, then it is possible to observe this memory effect.

ACKNOWLEDGMENTS

This work is supported by National Science Foundation of China Grant No. 11105091.

APPENDIX A: ANGULAR VELOCITY OF A FREE-FALLING GYROSCOPE

Given the metric ($i = 1, 2$):

$$g = 2dUdV + \delta_{ij}dX^i dX^j + DdU^2, \tag{A1}$$

where

$$D = K_{ij}(U)X^iX^j = \frac{1}{2}A_+(U)((X^1)^2 - (X^2)^2) + A_\times(U)X^1X^2, \tag{A2}$$

all nonzero components of affine connections and the curvature tensor are

$$\begin{aligned}
&\Gamma^1_{00} = \frac{1}{2}\partial_0 D, \qquad \Gamma^2_{00} = -K_{1a}X^a = -\frac{1}{2}\partial_2 D, \qquad \Gamma^3_{00} = K_{2a}X^a = -\frac{1}{2}\partial_3 D,\\
&\Gamma^1_{20} = \Gamma^1_{02} = K_{1a}X^a = \frac{1}{2}\partial_2 D, \qquad \Gamma^1_{30} = \Gamma^1_{03} = K_{2a}X^a = \frac{1}{2}\partial_3 D,\\
&R_{0i0j} = -K_{ij}, \qquad R_{00} = -K_{22} - K_{11}.
\end{aligned} \tag{A3}$$

The proper velocity is given by

$$\begin{aligned}
&\boldsymbol{u} = \gamma(1, v^1, v^a) \quad \text{with} \quad \boldsymbol{u}\cdot\boldsymbol{u} = -1 \quad \text{and}\\
&\gamma = (-D - 2v^1 - v^a v_a)^{-1/2}.
\end{aligned} \tag{A4}$$

Establish a local tetrad as

$$\begin{aligned}
\boldsymbol{e}_{\hat 0} &= \boldsymbol{u},\\
\boldsymbol{e}_{\hat 1} &= \frac{1}{\gamma}\boldsymbol{l} + \boldsymbol{u},\\
\boldsymbol{e}_{\hat a} &= \partial_a - v^a \boldsymbol{l},
\end{aligned} \tag{A5}$$

where $\boldsymbol{l} = \partial_V$ and $\partial_a = \partial_{X^a}$. Since the geodesic equation of U is $\frac{d^2U}{d\tau^2} = 0$, $\gamma =$ Constant. We first expand the spin connection $\omega_a^{\hat i \hat j} = \boldsymbol{e}^{\hat i}_\mu \nabla_a \boldsymbol{e}^{\hat j \mu}$, yielding

$$\begin{aligned}
\omega_\nu^{\hat i \hat j} = {} & \boldsymbol{e}_{\hat i}{}^0 D\partial_\nu \boldsymbol{e}^{\hat j 0} + \boldsymbol{e}_{\hat i}{}^0\partial_\nu \boldsymbol{e}^{\hat j 1} + \boldsymbol{e}_{\hat i}{}^1\partial_\nu \boldsymbol{e}^{\hat j 0} + \boldsymbol{e}_{\hat i}{}^2\partial_\nu \boldsymbol{e}^{\hat j 2} + \boldsymbol{e}_{\hat i}{}^3\partial_\nu \boldsymbol{e}^{\hat j 3}\\
& + \boldsymbol{e}_{\hat i}{}^0(\Gamma^1_{\nu 0}\boldsymbol{e}^{\hat j 0} + \Gamma^1_{\nu 2}\boldsymbol{e}^{\hat j 2} + \Gamma^1_{\nu 3}\boldsymbol{e}^{\hat j 3})\\
& + \boldsymbol{e}_{\hat i}{}^2\Gamma^2_{\nu 0}\boldsymbol{e}^{\hat j 0} + \boldsymbol{e}_{\hat i}{}^3\Gamma^3_{\nu 0}\boldsymbol{e}^{\hat j 0}.
\end{aligned} \tag{A6}$$

Then, by using the tetrad (A5), we obtain

$$\begin{aligned}
\omega_\nu^{\hat a \hat b} &= 0,\\
\omega_\nu^{\hat 1 \hat a} &= -\gamma\partial_\nu v^a + \gamma\Gamma^1_{\nu \mathrm{b}}\delta^{ab}.
\end{aligned} \tag{A7}$$

Comparing the geodesic equation (7) with Eq. (A3), we have

$$\ddot X^a = K^a_b X^b = -\Gamma^a_{00}, \tag{A8}$$

the only nonzero component of the spin connection is

$$\omega_0^{\hat 1 \hat a} = -\gamma \ddot X^a + \gamma\Gamma^1_{0a} = \gamma(\Gamma^a_{00} + \Gamma^1_{0a}) = 0, \tag{A9}$$

therefore, the angular velocity $\boldsymbol{\Omega}$ is equal to zero.

APPENDIX B: ANGULAR VELOCITY OF A STATIC GYROSCOPE

In asymptotically flat spacetimes, a static observer means he/she is static relative to the source, and he/she will observe a precession velocity of leading order $\mathcal{O}(1/r)$, which contains the same information as the standard displacement memory (see Sec. 4.3 of [17]).

In plane wave spacetimes, we consider an observer who is static relative to the origin of coordinates, this consideration is due to the fact that the origin point of plane wave spacetime is static relative to the source. We do the same calculation as in Appendix A: the four velocity that is relatively static to the origin reads $\boldsymbol{u} = \frac{1}{\sqrt{2}}(\partial_U - \partial_V)$, and the tetrad (A5) now becomes

$$\boldsymbol{e}_{\hat{0}} = \frac{1}{\sqrt{2}}(\partial_U - \partial_V),$$
$$\boldsymbol{e}_{\hat{1}} = \frac{1}{\sqrt{2}}(\partial_U - \partial_V) + \sqrt{2}\partial_V,$$
$$\boldsymbol{e}_{\hat{a}} = \partial_a, \tag{B1}$$

the spin connection is

$$\omega_\nu^{\hat{1}\,\hat{a}} = -\boldsymbol{e}_{\hat{1}}{}^0 \partial_\nu v^a + \boldsymbol{e}_{\hat{1}}{}^0 \Gamma^1_{\nu b}\delta^{ab} = \frac{1}{2\sqrt{2}}\partial_a D dU = \frac{1}{\sqrt{2}} K_{ab} X^b dU, \tag{B2}$$

and the nonvanishing component of the angular velocity is

$$\Omega_{\hat{1}\,\hat{a}} = -\frac{1}{2} K_{ab} X^b. \tag{B3}$$

Since $K_{ab} = -R_{aUbU}$, the angular velocity (B3) contains the same information as the standard displacement memory in plane wave spacetimes. The result is consistent with that in asymptotically flat spacetimes at order $\mathcal{O}(1/r)$ [17].

[1] P. D. Lasky, E. Thrane, Y. Levin, J. Blackman, and Y. Chen, Detecting Gravitational-Wave Memory with LIGO: Implications of GW150914, Phys. Rev. Lett. **117**, 061102 (2016).

[2] B. Abbott, R. Abbott, T. Abbott, M. Abernathy *et al.*, Observation of Gravitational Waves from a Binary Black Hole Merger, Phys. Rev. Lett. **116**, 061102 (2016).

[3] Y. B. Zel'dovich and A. G. Polnarev, Detecting Gravitational-Wave Memory with LIGO: Implications of GW150914, Phys. Rev. Lett. **117**, 061102 (2016).

[4] L. P. Grishchuk and A. G. Polnarev, Gravitationalwave pulseswith "velocity-coded memory", Zh. Eksp. Teor. Fiz. **96**, 1153 (1989) [Sov. Phys. JETP **69**, 653 (1989)].

[5] D. Christodoulou, Nonlinear Nature of Gravitation and Gravitational-Wave Experiments, Phys. Rev. Lett. **67**, 1486 (1991).

[6] A. G. Wiseman and C. M. Will, Christodoulou's nonlinear gravitational-wave memory: Evaluation in the quadrupole approximation, Phys. Rev. D **44**, R2945 (1991).

[7] M. Favata, Post-newtonian corrections to the gravitational-wave memory for quasicircular, inspiralling compact binaries, Phys. Rev. D **80**, 024002 (2009).

[8] L. Blanchet, Gravitational radiation from post-newtonian sources and inspiralling compact binaries, Living Rev. Relativity **17**, 2 (2014).

[9] M. Favata, Nonlinear gravitational-wave memory from binary black hole mergers, Astrophys. J. **696**, L159 (2009).

[10] K. Mitman, J. Moxon, M. A. Scheel, S. A. Teukolsky, M. Boyle, N. Deppe, L. E. Kidder, and W. Throwe, Computation of displacement and spin gravitational memory in numerical relativity., Phys. Rev. D **102**, 104007 (2020).

[11] M. Favata, The gravitational-wave memory effect, Classical Quantum Gravity **27**, 084036 (2010).

[12] P.-M. Zhang, C. Duval, G. W. Gibbons, and P. A. Horvathy, Soft gravitons and the memory effect for plane gravitational waves, Phys. Rev. D **96**, 064013 (2017).

[13] A. K. Divakarla and B. F. Whiting, The first-order velocity memory effect from compact binary coalescing sources, Phys. Rev. D **104**, 064001 (2021).

[14] S. Pasterski, A. Strominger, and A. Zhiboedov, New gravitational memories, J. High Energy Phys. 12 (2016) 053.

[15] D. A. Nichols, Spin memory effect for compact binaries in the post-Newtonian approximation, Phys. Rev. D **95**, 084048 (2017).

[16] D. A. Nichols, Center-of-mass angular momentum and memory effect in asymptotically flat spacetimes, Phys. Rev. D **95**, 084048 (2017).

[17] A. Seraj and B. Oblak, Gyroscopic gravitational memory, arXiv:2112.04535.

[18] E. E. Flanagan and D. A. Nichols, Conserved charges of the extended Bondi-Metzner-Sachs algebra, Phys. Rev. D **95**, 044002 (2017).

[19] R. Sachs, Asymptotic symmetries in gravitational theory, Phys. Rev. **128**, 2851 (1962).

[20] A. Strominger and A. Zhiboedov, Gravitational memory, BMS supertranslations and soft theorems, arXiv:1411.5745.

[21] A. Strominger, Lectures on the infrared structure of gravity and gauge theory, arXiv:1703.05448.

[22] A. Seraj and B. Oblak, The Precession Caused by Gravitational Waves, Phys. Rev. Lett. **129**, 061101 (2022).

[23] P. Mao and X. Wu, More on gravitational memory, J. High Energy Phys. 05 (2019) 058.

[24] A. I. Harte, Optics in a nonlinear gravitational plane wave, Classical Quantum Gravity **32**, 175017 (2015).

[25] E. E. Flanagan, A. M. Grant, A. I. Harte, and D. A. Nichols, Persistent gravitational wave observables: Nonlinear plane wave spacetimes, Phys. Rev. D **101**, 104033 (2020).

[26] P.-M. Zhang, M. Elbistan, G. W. Gibbons, and P. A. Horvathy, Sturm-liouville and carroll: At the heart of the memory effect, Gen. Relativ. Gravit. **50**, 107 (2018).

[27] G. Comp ere and A. Fiorucci, Advanced lectures on general relativity, arXiv:1801.07064.

[28] M. Godazgar, G. Long, and A. Seraj, Gravitational memory effects and higher derivative actions, J. High Energy Phys. 09 (2022) 150.

[29] E. E. Flanagan and D. A. Nichols, Observer dependence of angular momentum in general relativity and its relationship to the gravitational-wave memory effect, arXiv:1411.4599.
[30] O. M. Boersma, D. A. Nichols, and P. Schmidt, Forecasts for detecting the gravitational-wave memory effect with Advanced LIGO and Virgo, Phys. Rev. D **101**, 083026 (2020).
[31] R. Oliveri and S. Speziale, A note on dual gravitational charges, J. High Energy Phys. 12 (2020) 079.
[32] K.-X. Sun, M. M. Fejer, E. Gustafson, and R. L. Byer, Sagnac Interferometer for Gravitational-Wave Detection, Phys. Rev. Lett. **76**, 3053 (1996).
[33] P. Amaro-Seoane, H. Audley, S. Babak *et al.*, Laser interferometer space antenna, arXiv:1702.00786.
[34] D. A. Shaddock, Operating LISA as a sagnac interferometer, Phys. Rev. D **69**, 022001 (2004).